

Tolerogenic dendritic cells induced by atorvastatin via inhibition of the TLR-4/NF- κ B pathway improve cardiac remodeling after myocardial infarction

Jianbing Zhu

Department of Cardiology, The First Affiliated Hospital of Nanchang University, Nanchang, Jiangxi Province 330006, P.R. China.

Hang Chen

Heart Center of Fujian Province, Union Hospital, Fujian Medical University, 29 Xin-Quan Road, Fuzhou 350001, China.

Yuanji Ma

Department of Cardiology, Zhongshan Hospital, Fudan University, 180 Fenglin Road, Shanghai 200032, China.

Haibo Liu

Department of Cardiology, Zhongshan Hospital, Fudan University, 180 Fenglin Road, Shanghai 200032, China.

Zhaoyang Chen (✉ chenzhaoyang888@126.com)

Heart Center of Fujian Province, Union Hospital, Fujian Medical University, 29 Xin-Quan Road, Fuzhou 350001, China.

Research Article

Keywords: Tolerogenic DCs (tDCs), myocardial infarction, atorvastatin

Posted Date: December 15th, 2020

DOI: <https://doi.org/10.21203/rs.3.rs-118076/v1>

License:  This work is licensed under a Creative Commons Attribution 4.0 International License.

[Read Full License](#)

Abstract

Background

Necrosis of ischemic cardiomyocytes after myocardial infarction (MI) activates an intense inflammatory reaction. Dendritic cells (DCs) play a crucial role in the repair process after MI. Tolerogenic DCs (tDCs) can inhibit inflammatory responses.

Methods and results

We investigated the role of atorvastatin and supernatants of necrotic cardiomyocytes (SNC) on DCs. We found that SNC induced DCs maturation, activated TLR-4/NF- κ B pathway, promoted inflammatory cytokines secretion and oxidative stress. Co-treatment with SNC and atorvastatin suppressed DC maturation and inflammatory response, which meant that atorvastatin induced DCs tolerate to SNC. Then, we investigated the effect of mDCs induced by SNC and tDCs induced by atorvastatin on ventricular remodeling after MI. tDCs treatment significantly improved the left ventricular systolic function, reduced the infiltration of MPO⁺ neutrophil, Mac3⁺ macrophages and CD3⁺ T cells, inhibited myocardial apoptosis and fibrosis, and decreased infarct size. Compared with PBS, treatment with mDCs did not showed beneficial effect on ventricular remodeling and inflammatory reaction after MI in mice.

Conclusion

Atorvastatin inactivated the TLR-4/NF- κ B pathway, repressed the oxidative stress, inflammatory response, and immune maturity induced by SNC. Treatment with tDCs, induced by co-treated with atorvastatin, preserved left ventricular function, limited infarct size, suppressed the infiltration of inflammatory cells, and attenuated the severity of fibrosis, and reduced the number of apoptotic cardiomyocytes.

Introduction

Myocardial infarction (MI) remains the leading cause of death worldwide [1]. Necrosis of ischemic cardiomyocytes in the infarcted myocardium activates both myocardial and systemic inflammatory responses. For example, animal experiments have suggested that inflammatory cells infiltrating the infarcted myocardium may exacerbate an ischemic injury, causing the death of viable cardiomyocytes and adverse left ventricular remodeling. However, clinical trials examining anti-inflammatory approaches in patients with myocardial infarction did not improve outcomes and failed to reduce the size of the infarct [2].

In recent decades, new efforts have pursued therapeutic strategies aimed at exploiting stem cell biology in the preservation, regeneration, or repair of cardiac tissue post-MI. However, a recent meta-analysis assessing the results of stem cell therapy for patients with acute MI demonstrated no net beneficial effects on outcomes, except for a small improvement in the ejection fraction. Although some stem cells differentiate to express markers characteristic of cardiomyocytes, the majority of studies demonstrated

that the potential benefit derived from stem cells does not result from trans-differentiating into the target tissue but from their paracrine activities, such as secretion of several cytokines and growth factors related to the inhibition of inflammation and adverse left ventricular remodeling [3]. Thus, we put forward the hypothesis that the adoptive transfer of a specialized regulatory immune cell after MI may have better outcomes than stem cell therapy.

Dendritic cells (DCs) are the primary professional antigen-presenting cells, uniquely able to induce naïve T cell activation and effector differentiation. Accumulating evidence strongly suggests that DCs are much more versatile in their functions than previously thought [4]. For example, DCs have been identified as relevant sources of cytokines in the healing infarct. Additionally, our previous studies have suggested that the immune maturation of DCs may play a crucial role in atherosclerotic lesions and the repair process after MI [5–10]. We found that the supernatants of necrotic cardiomyocytes (SNCs) induced the maturation and inflammatory reaction of DCs [9–10]. Our previous study also demonstrated that atorvastatin inhibited Angiotensin II (AngII)-induced inflammatory responses via the downregulation of DC surface markers and inflammatory cytokines [11]. Thus, the goal of this study is to investigate the role of atorvastatin on DC maturation induced by SNCs, and the effect of treatment with DCs treated with atorvastatin after MI.

Materials And Methods

Simulation of post-MI cardiomyocyte microenvironment

Two types of samples were used to mimic the MI microenvironment: 1. the supernatants of necrotic HL-1 cells (Supernatant-NH), 2. the supernatants of infarcted myocardium (Supernatant-IM) at 8 h post-MI. The generation of necrotic HL-1 cells was performed according to the protocol described by Maekawa et al. [12]. Briefly, HL-1 (a cardiac muscle cell line; SXBIO, Shanghai, China) cells were washed three times with serum-free medium and then processed by five cycles of freezing in liquid nitrogen followed by thawing at 37 °C. Supernatants from infarcted mouse myocardium were obtained from MI-model mice after ligation of the left anterior descending (LAD) artery for 8 h. In brief, the hearts of the mice were removed under sterile conditions, and sections of infarcted myocardium were excised and washed three times in phosphate-buffered saline (PBS) to remove blood cells. Following this, the sections were cut into small pieces that were used to generate single-cell suspensions via the gentleMACS™ system (MACS® Cell Separation, Miltenyi Biotec B.V.& Co., Bergisch Gladbach, Germany). Finally, the supernatants were obtained by centrifugation. Then, 100-µL samples (cell membrane particles were removed by centrifugation at 1500 g for 30 min) were collected from the supernatants of the HL-1 cells, and infarcted myocardial cells were added to 10⁶ bone marrow-derived dendritic cells (BMDCs) for 24 h. All experiments were performed under sterile conditions. All procedures performed in studies involving animals were in accordance with the ethical standards of Laboratory Animal Management and experimental ethics committee of Union Hospital, Fujian Medical University. All methods were performed in accordance with relevant guidelines and regulations.

Cell culture and treatments

The BMDCs obtained from approximately 6-week-old C57BL/6 mice were cultured in RPMI 1640 Media supplemented with 10 ng/mL granulocyte-macrophage colony-stimulating factor (GM-CSF) and 1 ng/mL IL-4 at 37 °C in 5% humidified CO₂ for 4 h. The medium containing nonadherent cells was replaced with fresh medium every 2 d. On culture day 7, the cells were treated with Supernatant-NH and Supernatant-IM alone, or in combination with 10 μM atorvastatin (Sigma-Aldrich, St. Louis, MO, USA) for 24 h. PBS was used as a control.

Induction of MI models and injection of DCs

Ligation of the left main descending coronary artery (LCA) was performed as described previously [9]. In brief, mice were anesthetized with 2% isoflurane, and their hearts were manually exposed through small chest incisions. The LCA was permanently ligated with a 7–0 silk suture 2–3 mm from the origin of the left atrium. The ligations were validated as successful by characteristic ECG changes. For the DCs transfer experiment, 1×10⁶ DCs treated with Supernatant-IM (mature DCs, mDCs), 1×10⁶ DCs treated with atorvastatin and Supernatant-IM (tolerogenic DCs, tDCs), and PBS were infused intravenously 1 d before and 1 week after MI.

Flow cytometric measurement

BMDCs were washed and resuspended in ice-cold PBS containing 5% fetal bovine serum (FBS) to prevent nonspecific binding, and further incubated with anti-CD80, anti-CD86, and anti-CD40 (BD Pharmingen, San Diego, CA, USA) for 30 min at 4 °C. After extensive washing, the stained cells were analyzed using a FACScan™ flow cytometer (BD Biosciences, San Jose, CA, USA) and CellQuest™ software (BD Biosciences, San Jose, CA, USA).

Intracellular levels of reactive oxygen species (ROS) were measured with DCFH-DA molecular probes (Molecular Probes-Invitrogen, Carlsbad, CA, USA). Cells were incubated with 10 μM DCFH-DA for 30 min at 37 °C, then washed and resuspended in PBS at 1 × 10⁶ cells/mL. The DCs were analyzed using flow cytometry. The fluorescence was determined at 503/529 nm and expressed as a percentage of the control.

Enzyme-linked immunosorbent assay

The supernatant of the cultured BMDCs was harvested and stored at –70 °C. The cytokine concentrations of TNF-α, IL-1, IL-6, IL-12P40, and IL-8 were analyzed using enzyme-linked immunosorbent assay (ELISA) kits (R&D Systems, Inc., Minneapolis, MN, USA) according to the manufacturer's instructions. The superoxide dismutase (SOD) activity and malondialdehyde (MDA) contents were measured at 450 and 532 nm by SOD and MDA ELISA kits (R&D Systems, Inc., Minneapolis, MN, USA), respectively.

Western blotting

Protein samples were fractionated with 12% SDS-PAGE (Invitrogen, Carlsbad, CA, USA) and transferred to polyvinylidene fluoride membranes (Millipore, Bedford, MA, USA). The membranes with blotted protein were blocked, then probed with the following antibodies: toll-like receptor 4 (TLR-4), nuclear factor- κ B (NF- κ B), phospho-NF- κ B, I κ B, phospho-I κ B, interleukin-1 receptor-associated kinase 4 (IRAK4), and phospho-IRAK4 at 4 °C overnight (Cell Signal Technology, Inc., Danvers, MA, USA). The membranes were washed and incubated at 4 °C for 2 h with diluted (1:5000) secondary HRP-conjugated antibodies.

Immunoreactive proteins were identified using Super Signal West Pico Chemiluminescent Substrate (Thermo Fisher Scientific, Franklin, MA, USA). Densitometric analysis of the western blotting was performed using Image J software.

Echocardiography

In vivo cardiac function was determined by echocardiography using the Vevo[®] 2100 Imaging Platform (VisualSonics, Inc., Toronto, Canada) as described previously [9]. Briefly, the mice were anesthetized with 2% isoflurane and oxygen, and two-dimensional echocardiographic views of the left ventricular long axis through the anterior and posterior LV walls were obtained at the level of the papillary muscle tips below the mitral valve. The left ventricular ejection fraction (LVEF) and fractional shortening (FS) were calculated as previously reported [6]. The echocardiograms were evaluated in a blinded manner.

Measurement of myocardial infarct size and myocardial fibrosis

After freezing at -20 °C for 12 hours, the heart ventricles were sectioned transversely into ~2-mm thick sections. The sections were subsequently incubated in 1% triphenyltetrazolium chloride (TTC) for 15 min at 37 °C to identify the non-infarcted and infarcted areas. Once identified, the areas were fixed in 10% buffered formalin. The infarcted area was displayed as the TTC-unstained area (white). The extent of fibrosis was measured using Masson's trichrome stain on day 28 after MI. Image-Pro Plus software (v6.0; Media Cybernetics, Rockville, MD, USA) was used to determine the infarct size and extent of fibrosis.

Immunohistochemistry analysis

Immunohistochemical studies were performed by immunoperoxidase staining methods using paraffin-embedded tissue sections (6 mm thick). After inhibiting endogenous peroxidase activity, the sections were incubated with primary anti-myeloperoxidase (MPO; Abbiotec[™], Midlothian, UK), anti-Mac3 (BD Biosciences, San Jose, CA, USA), and anti-CD3 (eBioscience, Inc., San Diego, CA, USA) at 4 °C overnight, followed by respective secondary HRP-conjugated antibodies for 1 h at room temperature. The positive cells were visualized with DAB, and nuclei were counterstained with hematoxylin. The numbers of Mac3+ macrophages, MPO+ neutrophils, and CD3+ T lymphocytes were assessed by counting the total cell numbers in the infarcted and border areas in twenty randomly chosen fields in each section.

Cardiomyocyte apoptosis

Cardiomyocyte apoptosis was assessed in the heart sections by terminal deoxynucleotidyl transferase-mediated dUTP nick-end-labeling (TUNEL) staining. TUNEL staining was performed using the *In situ* Cell Death Detection Kit (Roche Applied Science, Upper Bavaria, Germany) according to the manufacturer's protocol. The apoptosis index was determined by counting TUNEL-positive nuclei in ten random fields per section and expressed as a percentage of the total nuclei.

Statistical analyses

The data are presented as the means \pm SD, with $P < 0.05$ considered to be statistically significant. A one-way ANOVA, followed by the Student-Newman-Keuls (SNK) test, was employed for the statistical analysis of our results. All statistical analyses were performed with SPSS 21 statistical software.

Results

Effect of atorvastatin on DCs maturation and inflammatory cytokine secretion

There were several observable costimulatory proteins on the surface of BMDCs, including CD40, CD80, and CD86. These proteins were examined in DCs that were treated with Supernatant-NH and Supernatant-IM alone, or in combination with 10 μ M atorvastatin. The flow cytometry results showed that Supernatant-NH and Supernatant-IM upregulated the expression of the cell-surface markers CD40, CD80, and CD86. We subsequently observed that atorvastatin significantly downregulated CD40, CD80, and CD86. These results indicate that atorvastatin may suppress DC maturation induced by Supernatant-NH and Supernatant-IM (Fig. 1).

An analysis of cytokine levels, that is, TNF- α , IL-1, IL-6, IL-12P40, and IL-8, indicated an inflammatory response, which was induced by Supernatant-NH and Supernatant-IM in DCs. We found that the secretion of TNF- α , IL-1, IL-6, IL-12P40, and IL-8 was increased significantly in the presence of Supernatant-NH and Supernatant-IM. In addition, the secretion of these cytokines was suppressed by atorvastatin (Fig. 1).

Atorvastatin attenuates oxidative stress in DCs

To investigate how atorvastatin affects the oxidative stress in DCs induced by Supernatant-NH and Supernatant-IM, we used flow cytometry to measure the intracellular level of ROS in response to Supernatant-NH and Supernatant-IM stimulation. Moreover, we also measured the levels of MDA and SOD with ELISA kits. As depicted in Figure 2, Supernatant-NH and Supernatant-IM exhibited a stimulating effect on ROS and MDA production but inhibited SOD activity. Cotreatment with atorvastatin reduced intracellular ROS production, and similar results were observed with MDA. However, atorvastatin suppressed the inhibition of SOD activity induced by Supernatant-NH and Supernatant-IM. Therefore, these results suggest that atorvastatin significantly suppresses oxidative stress in DCs induced by Supernatant-NH and Supernatant-IM.

Atorvastatin inactivates the TLR-4/NF- κ B pathway

To investigate how atorvastatin affects the TLR-4/NF- κ B pathway, we used western immunoblotting to measure the expression of TLR-4 and the phosphorylation of IRAK4, NF- κ B, and I κ B. It was found that Supernatant-NH and Supernatant-IM increased TLR-4 expression and phosphorylation of IRAK4, NF- κ B, and I κ B. Additionally, atorvastatin inactivated the TLR-4/NF- κ B pathway induced by Supernatant-NH and Supernatant-IM (Figure 3).

Effect of DCs transfer on the survival and LV function in MI mice

As demonstrated above, Supernatant-IM induced DC maturation, activated inflammatory signal pathways, promoted inflammatory cytokine secretion, and oxidative stress. Nonetheless, co-treatment with atorvastatin suppressed DC maturation and inflammatory cytokine secretion, inactivated the TLR-4/NF- κ B pathway, suggesting that atorvastatin induced DCs to tolerate Supernatant-IM. Therefore, we investigated the effect of mDCs induced by Supernatant-IM, tolerogenic DCs (tDCs) induced by Supernatant-IM, and atorvastatin co-treatment on the survival and LV function in MI mice.

Compared to PBS and mDCs treatment after MI, tDCs treatment significantly improved the LVEF at 4 weeks after MI. Both the LVEDD and LVESD were reduced in tDCs treatment mice. The survival rate trended towards being higher in the tDCs-treated mice compared with the PBS- and mDCs-treated mice on day 28. No beneficial effects on cardiac function were observed in the mDCs group. These findings demonstrated that tDCs treatment might attenuate adverse remodeling and improve LV systolic function (Figure 4).

Effect of DCs transfer on the inflammatory reaction after MI

Immunohistochemical staining for MPO showed that the number of neutrophils that infiltrated into the infarcted myocardium was significantly reduced in the tDCs group at 3 and 7 d after MI than in the PBS and mDCs group. Similarly, tDCs treatment significantly decreased Mac3⁺ macrophage infiltration compared to the PBS and mDCs group. The number of CD3⁺ T cells that infiltrated the infarcted myocardium was also downregulated in the tDCs group. Compared with the PBS group, mDCs treatment did not reduce the infiltration of inflammatory cells into the infarcted heart (Figure 5).

Effect of DCs transfer on infarct size, apoptosis, and fibrosis in MI mice

The number of myocardial apoptotic nuclei, as detected by TUNEL staining, was significantly lower in the LV border zone of tDCs treatment mice compared with PBS and mDCs treatment mice on day 3 after MI. TTC staining on the first day after MI demonstrated a significantly smaller infarct size in the tDCs group. On day 28, Masson's trichrome staining showed that tDCs treatment significantly reduced LV fibrosis. On the contrary, mDCs treatment did not show a reduction in apoptosis, infarct size, or fibrosis. (Figure 6).

Discussion

The initial finding of our study is that atorvastatin inactivated the TLR-4/NF- κ B pathway as well as repressed the inflammatory response, oxidative stress, and immune maturity induced by SNCs. Secondly,

treatment with tDCs, which were induced by co-treatment with atorvastatin and SNCs, preserved left ventricular function, limited the infarct size, suppressed the infiltration of inflammatory cells, attenuated the severity of fibrosis, and reduced the number of apoptotic cardiomyocytes.

DCs are antigen-presenting cells that are highly involved in the process of myocardial infarction [13]. Ferrans et al. demonstrated the rapid accumulation of interstitial DCs in the border zones 7 d after myocardial infarction (left coronary artery ligation) in the rat heart. DCs tend to be assembled in small clusters with CD4⁺ T cells, which disappear 21 d after coronary ligation [14]. Anzai and colleagues reported that selective depletion of DCs exacerbated post-infarction LV remodeling in association with enhanced inflammatory cytokine expression, inducible nitric oxide synthase production, and MMP-9 activation [15]. Furthermore, the cardioprotective effects of ACEI were enhanced through attenuating migration of DCs from the spleen into peripheral circulation, thereby inhibiting DCs maturation and tissue inflammation [16]. Toll-like receptors (TLRs) are a family of pattern recognition receptors expressed on DCs. Numerous studies have demonstrated that TLR4 activates the expression of several pro-inflammatory cytokine genes and induces immune maturity in DCs [17]. Recent studies have supported the notion that TLR4 of the bone marrow-derived cells plays an essential role in mediating cardiac dysfunction under certain pathological conditions [18].

In our previous studies, we used SNCs to simulate the post-MI cardiomyocyte micro-environment *in vitro*. We demonstrated that necrotic supernatants up-regulated the expression of DC maturation markers, and increased the levels of inflammatory cytokines [9, 10]. In the present study, we found that SNCs activated the TLR-4/NF- κ B pathway as well as induced the inflammatory response, oxidative stress, and immune maturity.

Statins, the cornerstone of antiatherogenic therapy, possess pleiotropic effects, including improved endothelial dysfunction, increased nitric oxide bioavailability and antioxidant properties, inhibition of inflammatory processes, and stabilization of atherosclerotic plaques [19]. In a previous study, we demonstrated that atorvastatin inhibited AngII-induced inflammatory responses via the downregulation of DC surface markers and inflammatory cytokines [11]. In this study, we showed that atorvastatin inactivated the TLR-4/NF- κ B pathway, repressed the inflammatory response, and immune maturity induced by SNCs.

DCs exist in an immature and mature state. Immature or semi-mature DCs can induce tolerance, also known as tDCs. Several studies have investigated a number of methodologies for inducing tDCs and the treatment effect on a variety of diseases [20]. It has been documented that tDCs, generated by using vitamin D₃, showed a stable maturation-resistant semi-mature phenotype with a low expression of activating co-stimulatory molecules as well as no production of the IL-12 family of cytokines. Furthermore, several studies demonstrated that tDCs induced by vitamin D₃ decreased islet rejection in pancreatic islet transplantation and prolonged male skin grafts in female recipients [21]. Vitamin D₃, dexamethasone, and rapamycin are also used to induce tolerogenic DCs, which are being further

investigated in animal experiments for organ transplantation rejection and certain inflammatory diseases [20].

Recently, several studies have also reported on the results of tDCs treatment for MI. Zhu and colleagues demonstrated that the adoptive transfer of IL-37 plus troponin–treated tDCs attenuated the infiltration of inflammatory cells in infarct hearts, decreased myocardial fibrosis, and improved cardiac function [22]. Choo and colleagues showed that subcutaneously administered tDCs resulted in better wound remodeling, preserved left ventricular systolic function after myocardial tissue damage, and improved survival [23]. In the present study, we found that atorvastatin inhibited the inflammatory response and immune maturity of DCs treated with SNCs. Therefore, we investigated the treatment effect of tDCs induced by atorvastatin and SNCs in MI mice, and found that tDCs preserved left ventricular function, limited infarct size, suppressed the infiltration of inflammatory cells, attenuated the severity of fibrosis, and reduced the number of apoptotic cardiomyocytes.

Conclusions

The present study demonstrated that atorvastatin inactivated the TLR-4/NF- κ B pathway, inhibited the immune maturity induced by SNCs. Furthermore, the adoptive transfer of tDCs induced by co-culturing with atorvastatin and SNCs preserved left ventricular function, limited infarct size, suppressed the infiltration of inflammatory cells, attenuated the severity of fibrosis, and reduced the number of apoptotic cardiomyocytes.

Declarations

Ethics approval and consent to participate The study design was approved by the ethics committee of Union Hospital, Fujian Medical University. All procedures performed in studies involving animals were in accordance with the ethical standards of Laboratory Animal Management and experimental ethics committee of Union Hospital, Fujian Medical University. All methods were performed in accordance with relevant guidelines and regulations.

Consent for publication All the authors have approved the manuscript and have agreed to submission to your esteemed journal. This manuscript has not been published or presented elsewhere in part or in its entirety, and is not under consideration by another journal.

Availability of data and materials All data generated or analysed during this study are included in this published article.

Competing interests The authors declare that there are no conflicts of interest.

Funding This study was supported by National Natural Science Foundation of China (Grant No. 81800324, and 81960061), National Natural Science Foundation of China (Grant No.81600241), Key Project of Science and Technology Research Funds of Department of Education of

Jiangxi Province(Grant No.GJJ170005), Natural Science Foundation of Jiangxi Province(Grant No. 20192ACBL21040) and Science and Technology Project of Jiangxi Provincial Health Commission Grant No. 20203094.

Authors' contributions Jianbing Zhu and Hang Chen performed the experiment and wrote the manuscript. Yuanji Ma and Haibo Liu analyzed the data. Zhaoyang Chen designed the the experiment.

Acknowledgements This study was supported by National Natural Science Foundation of China (Grant No. 81800324, and 81960061), National Natural Science Foundation of China(Grant No.81600241), Key Project of Science and Technology Research Funds of Department of Education of Jiangxi Province(Grant No.GJJ170005), Natural Science Foundation of Jiangxi Province(Grant No. 20192ACBL21040) and Science and Technology Project of Jiangxi Provincial Health Commission Grant No. 20203094.

References

1. Benjamin EJ, Virani SS, Callaway CW, et al. American Heart Association Council on Epidemiology and Prevention Statistics Committee and Stroke Statistics Subcommittee. Heart Disease and Stroke Statistics-2018 Update: A Report From the American Heart Association. *Circulation*. 2018;137(12):e67-e492.
2. Huang S, Frangogiannis NG. Anti-inflammatory therapies in myocardial infarction: failures, hopes and challenges. *Br J Pharmacol*. 2018;175(9):1377–1400.
3. Stempien-Otero A, Helterline D, Plummer T, et al. Mechanisms of bone marrow-derived cell therapy in ischemic cardiomyopathy with left ventricular assist device bridge to transplant. *J Am Coll Cardiol*. 2015;65(14):1424–34.
4. Maja-Theresa Dieterlen, Katja John, Hermann Reichenspurner, Friedrich W Mohr, Markus J Barten. Dendritic Cells and Their Role in Cardiovascular Diseases: A View on Human Studies. *J Immunol Res*. 2016;2016:5946807.
5. Ge J, Jia Q, Liang C, et al. Advanced glycosylation end products might promote atherosclerosis through inducing the immune maturation of dendritic cells. *Arterioscler Thromb Vasc Biol*. 2005;25(10):2157–63.
6. Huang D, Lu H, Liu H, et al. Losartan attenuates human monocyte-derived dendritic cell immune maturation via downregulation of lectin-like oxidized low-density lipoprotein receptor-1. *J Cardiovasc Pharmacol*. 2012;60(2):133–9.
7. Wu C, Gong Y, Yuan J, et al. microRNA-181a represses ox-LDL-stimulated inflammatory response in dendritic cell by targeting c-Fos. *J Lipid Res*. 2012; 53(11): 2355–63.
8. Zhu H, Jin X, Zhao J, et al. Probucol Protects Against Atherosclerosis Through Lipid-lowering and Suppressing Immune Maturation of CD11c + Dendritic Cells in STZ-induced Diabetic LDLR^{-/-} Mice. *J Cardiovasc Pharmacol*. 2015;65(6):620–7.

9. Liu H, Gao W, Yuan J, et al., Exosomes derived from dendritic cells improve cardiac function via activation of CD4(+) T lymphocytes after myocardial infarction. *J Mol Cell Cardiol.* 2016; 91:123–33.
10. Zhu J, Yao K, Guo J, et al. miR-181a and miR-150 regulate dendritic cell immune inflammatory responses and cardiomyocyte apoptosis via targeting JAK1-STAT1/c-Fos pathway. *J Cell Mol Med.* 2017;21(11):2884–2895.
11. Ma Y, Chen Z, Zou Y, Ge J. Atorvastatin represses the angiotensin 2-induced oxidative stress and inflammatory response in dendritic cells via the PI3K/Akt/Nrf 2 pathway. *Oxid Med Cell Longev.* 2014; 2014:148798.
12. Maekawa Y, Mizue N, Chan A, et al. Survival and cardiac remodeling after myocardial infarction are critically dependent on the host innate immune interleukin-1 receptor-associated kinase-4 signaling: a regulator of bone marrow-derived dendritic cells. *Circulation.* 2009; 120(14):1401–14.
13. Christ A, Temmerman L, Legein B, Daemen MJ, Biessen EA. Dendritic cells in cardiovascular diseases: epiphenomenon, contributor, or therapeutic opportunity. *Circulation.* 2013; 128(24):2603–13.
14. Zhang J, Yu ZX, Fujita S, Yamaguchi ML, Ferrans VJ. Interstitial dendritic cells of the rat heart. Quantitative and ultrastructural changes in experimental myocardial infarction. *Circulation.* 1993; 87(3):909–920.
15. Anzai A, Anzai T, Nagai S, et al. Regulatory role of dendritic cells in postinfarction healing and left ventricular remodeling. *Circulation.* 2012;125(10):1234–45.
16. Yuanji Ma, Jie Yuan, Jialu Hu, et al. ACE inhibitor suppresses cardiac remodeling after myocardial infarction by regulating dendritic cells and AT 2 receptor-mediated mechanism in mice. *Biomed Pharmacother.* 2019;114:108660.
17. Watts C, West MA, Zaru R. TLR signalling regulated antigen presentation in dendritic cells. *Curr Opin Immunol.* 2010;22(1):124–30.
18. Tavener SA, Long EM, Robbins SM, McRae KM, Van Remmen H, Kubes P. Immune cell Toll-like receptor 4 is required for cardiac myocyte impairment during endotoxemia. *Circ Res.* 2004;95(7):700–7.
19. Oesterle A, Laufs U, Liao JK. Pleiotropic Effects of Statins on the Cardiovascular System. *Circ Res.* 2017;120(1):229–243.
20. Gordon JR, Ma Y, Churchman L, Gordon SA, Dawicki W. Regulatory dendritic cells for immunotherapy in immunologic diseases. *Front Immunol.* 2014; 5:7.
21. Nikolic T, Roep BO. Regulatory multitasking of tolerogenic dendritic cells - lessons taken from vitamin d3-treated tolerogenic dendritic cells. *Front Immunol.* 2013;4:113.
22. Zhu R, Sun H, Yu K, et al. Interleukin-37 and Dendritic Cells Treated With Interleukin-37 Plus Troponin I Ameliorate Cardiac Remodeling After Myocardial Infarction. *J Am Heart Assoc.* 2016;5(12):e004406.
23. Choo EH, Lee JH, Park EH, et al. Infarcted Myocardium-Primed Dendritic Cells Improve Remodeling and Cardiac Function After Myocardial Infarction by Modulating the Regulatory T Cell and Macrophage Polarization. *Circulation.* 2017;135(15):1444–1457.

Figures

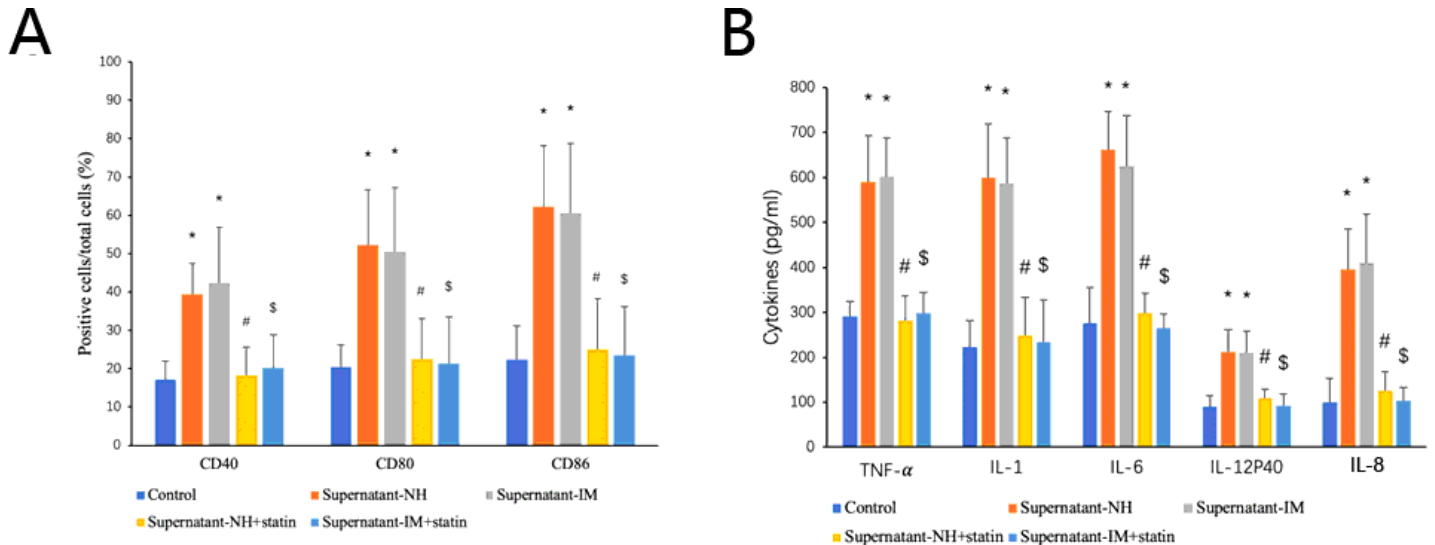


Figure 1

: The inhibitory effects of atorvastatin on bone marrow derived dendritic cell (BMDC) maturation and inflammatory responses induced by supernatant-NH and supernatant-IM. After pretreatment with phosphate-buffered saline (PBS), supernatant-NH, or supernatant-IM, BMDCs were exposed to atorvastatin for 24 h. (a) Expression of the cell- surface markers CD40, CD80, and CD86, as determined by flow cytometry ($n = 5$). (b) Expression of cytokines in BMDCs analyzed by ELISA ($n = 5$). The data are shown as the mean \pm (SD) ($n = 5$); * $P < 0.05$ versus control; # $P < 0.05$ versus supernatant-NH, \$ $P < 0.05$ versus supernatant-IM.

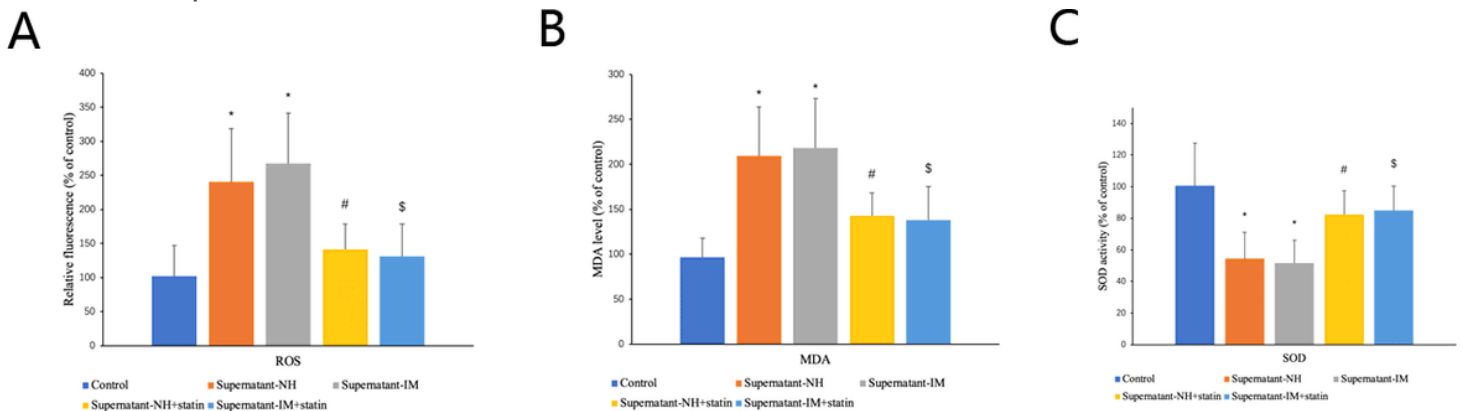


Figure 2

The effects of atorvastatin on reactive oxygen species (ROS) formation (a), malondialdehyde (MDA) levels (b), and superoxide dismutase (SOD) activity (c) in BMDCs in the presence of supernatant-NH and supernatant-IM. (a) The intracellular ROS levels were measured via flow cytometry using DCFH-DA. (b) The SOD activity and (c) MDA levels were measured at 450 and 532 nm, respectively, using ELISA kits.

The data are shown as the mean \pm (SD) ($n=5$); * $P < 0.05$ versus control; # $P < 0.05$ versus supernatant-NH, \$ $P < 0.05$ versus supernatant-IM.

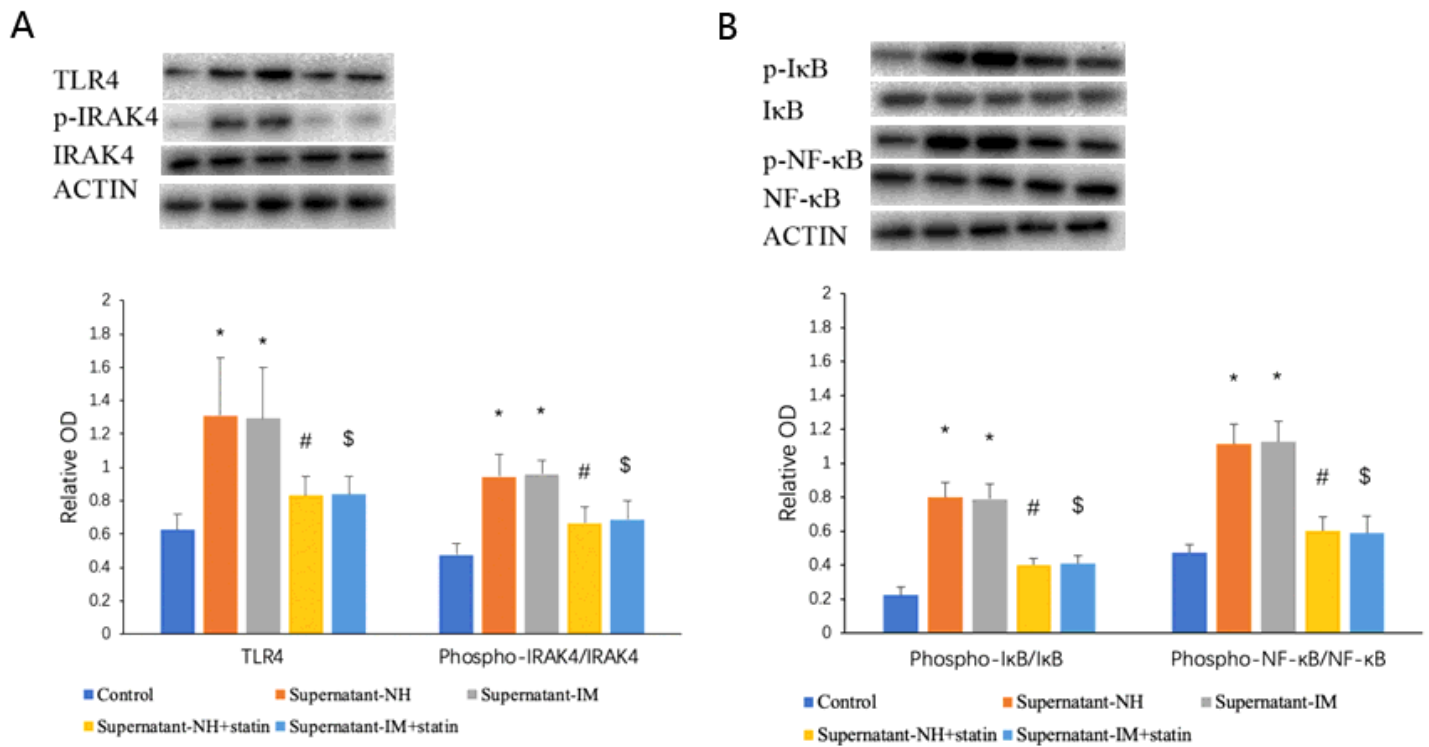


Figure 3

The effect of atorvastatin on the TLR-4/NF-κB pathway (a), effect of atorvastatin on the expression of TLR4 and phosphorylation of IRAK4. (b), effect of atorvastatin on the phosphorylation of NF-κB and IκB. * $P < 0.05$ versus control; # $P < 0.05$ versus supernatant-NH, \$ $P < 0.05$ versus supernatant-IM.

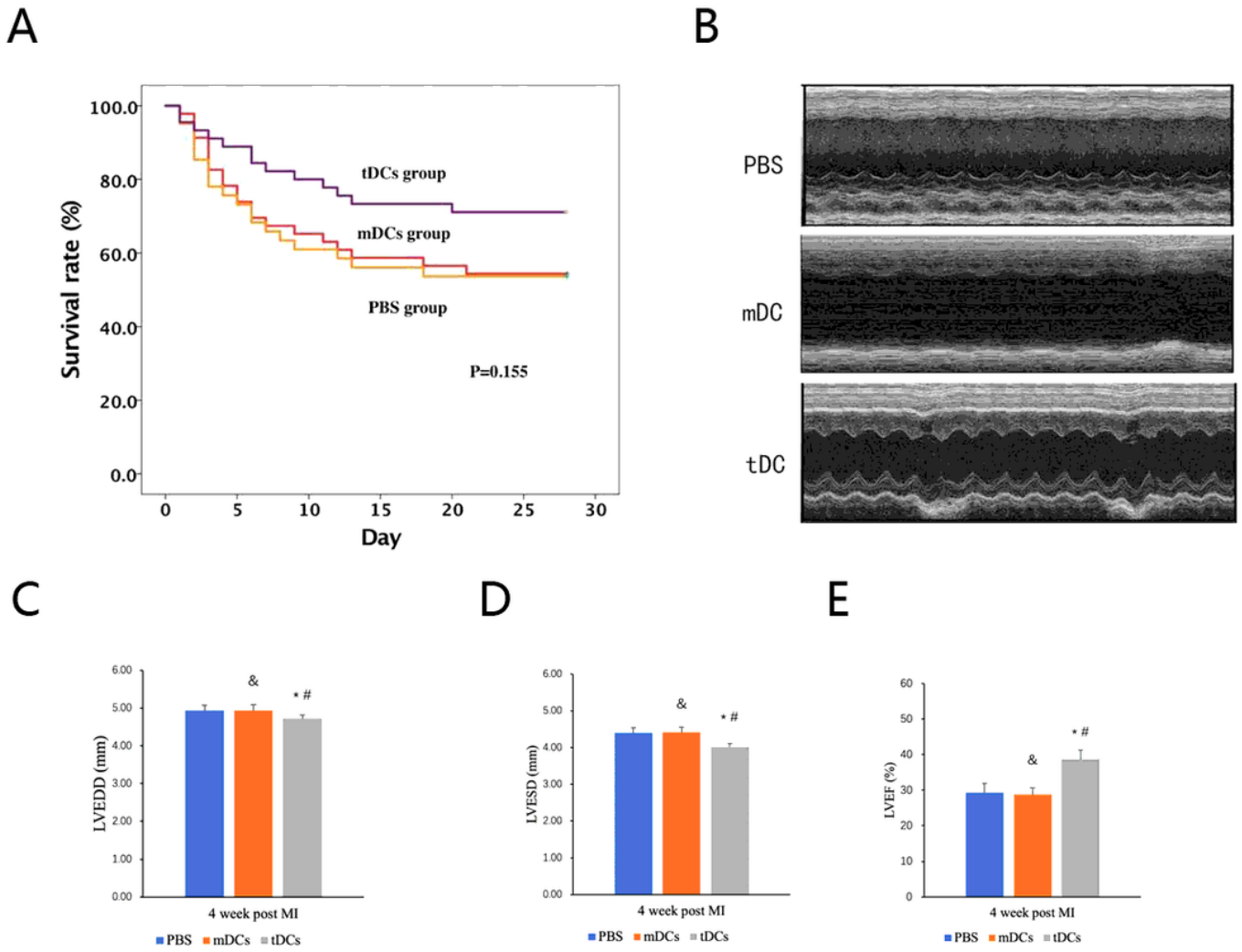
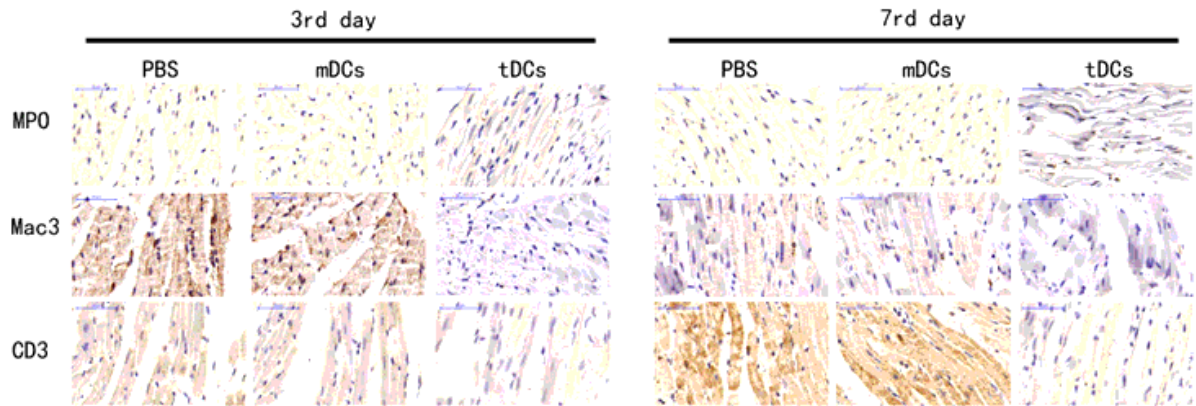


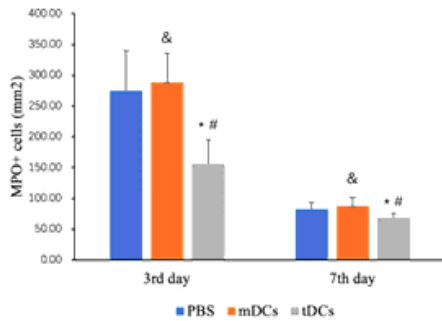
Figure 4

The effect of dendritic cell (DC) transfer on the survival (a), representative images of echocardiography (b), and LV function in MI mice (c, d, and e). * $P < 0.05$ versus PBS group; # $P < 0.05$ versus mature dendritic cells (mDCs) group, & $P < 0.05$ versus PBS group.

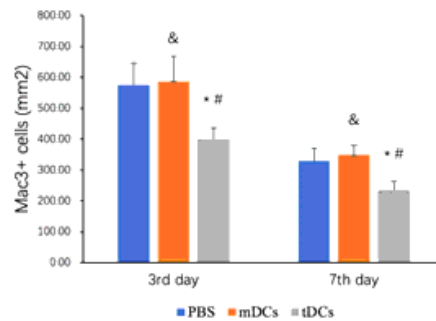
A



B



C



D

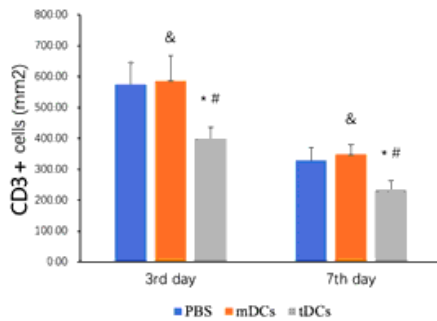


Figure 5

Reduced infiltration of inflammatory MPO+ neutrophil, Mac3+ macrophages and CD3+ T cells in the tDCs group compared with the PBS and mDCs groups in the border areas after MI. (a), Representative photographs of immunohistochemical staining for MPO+ neutrophil, Mac3+ macrophages 3 d, and CD3+ T cells, 3 d and 7 d after MI. (b), Time course of MPO+ neutrophil infiltration after MI. (c), Time course of Mac3+ macrophages infiltration after MI. (d), Time course of CD3+ T cells infiltration after MI. The data are shown as the mean \pm (SD) ($n = 5$); * $P < 0.05$ versus PBS group; # $P < 0.05$ versus mDCs group, & $P < 0.05$ versus PBS group.

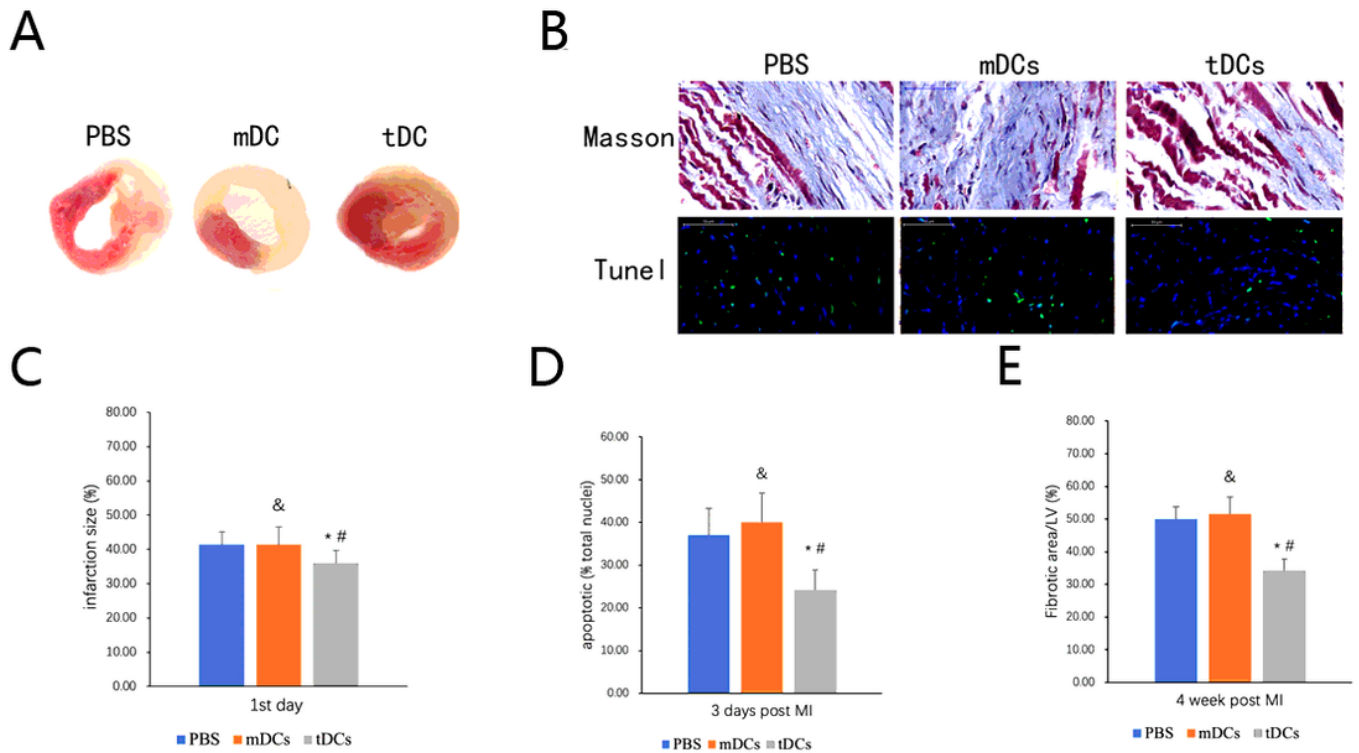


Figure 6

The effect of tDCs and mDCs treatment on the myocardial infarction size, fibrosis, and cardiomyocyte apoptosis in mice hearts after MI. (a), Representative images of TTC in the heart. (b), Representative images of cardiomyocyte apoptosis (Green, TUNEL-positive nuclei; Blue, DAPI-stained nuclei) and Masson's trichrome staining in the heart. (c), Effect of tDCs and mDCs treatment on myocardial infarction size on day 1 after MI. (d), Effect of tDCs and mDCs treatment on apoptosis. (e), Effect of tDCs and mDCs treatment on fibrosis. * $P < 0.05$ versus PBS group; # $P < 0.05$ versus mDCs group, & $P > 0.05$ versus PBS group.